OXFORD

Relation of Quantitative Histologic and Radiologic Breast Tissue Composition Metrics With Invasive Breast Cancer Risk

Mustapha Abubakar (iD), MD, PhD, [1,*] Shaoqi Fan (iD), MPH, [1] Erin Aiello Bowles (iD), MPH, [2] Lea Widemann, BS, [1] Máire A. Duggan (iD), MD, FRCPC, [3] Ruth M. Pfeiffer, PhD, [1] Roni T. Falk (iD), MS, [1] Scott Lawrence, MS,[4] Kathryn Richert-Boe, MD, [5] Andrew G. Glass, MD, [5,†] Teresa M. Kimes, MS, [5] Jonine D. Figueroa (iD), PhD, MPH, [6] Thomas E. Rohan, MBBS, PhD, [7,‡] Gretchen L. Gierach (iD) PhD, MPH[1,‡]

[1]Division of Cancer Epidemiology and Genetics, National Cancer Institute, National Institute of Health, USA, [2]Kaiser Permanente Washington Health Research Institute, Seattle, WA, USA, [3]Department of Pathology and Laboratory Medicine, University of Calgary, Calgary, Alberta, Canada, [4]Molecular and Digital Pathology Laboratory, Cancer Genomics Research Laboratory, Leidos Biomedical Research, Inc, Frederick, MD, USA, [5]Kaiser Permanente Center for Health Research, Portland, OR, USA, [6]Usher Institute of Population Health Sciences and Informatics, The University of Edinburgh, Scotland, UK and [7]Department of Epidemiology and Population Health, Albert Einstein College of Medicine, Bronx, NY, USA

*Correspondence to: Mustapha Abubakar, MD, PhD, Division of Cancer Epidemiology and Genetics, National Cancer Institute, National Institute of Health, 9609 Medical Center Drive, Rockville, MD, USA (e-mail: mustapha.abubakar2@nih.gov).
†Deceased.
‡Co-senior authors.

Abstract

Background: Benign breast disease (BBD) is a strong breast cancer risk factor, but identifying patients that might develop invasive breast cancer remains a challenge. **Methods:** By applying machine-learning to digitized hematoxylin and eosin–stained biopsies and computer-assisted thresholding to mammograms obtained circa BBD diagnosis, we generated quantitative tissue composition metrics and determined their association with future invasive breast cancer diagnosis. Archival breast biopsies and mammograms were obtained for women (18-86 years of age) in a case-control study, nested within a cohort of 15 395 BBD patients from Kaiser Permanente Northwest (1970-2012), followed through mid-2015. Patients who developed incident invasive breast cancer (ie, cases; n = 514) and those who did not (ie, controls; n = 514) were matched on BBD diagnosis age and plan membership duration. All statistical tests were 2-sided. **Results:** Increasing epithelial area on the BBD biopsy was associated with increasing breast cancer risk (odds ratio [OR]$_{Q4 vs Q1}$ = 1.85, 95% confidence interval [CI] = 1.13 to 3.04; P_{trend} = .02). Conversely, increasing stroma was associated with decreased risk in nonproliferative, but not proliferative, BBD ($P_{heterogeneity}$ = .002). Increasing epithelium-to-stroma proportion (OR$_{Q4 vs Q1}$ = 2.06, 95% CI =1.28 to 3.33; P_{trend} = .002) and percent mammographic density (MBD) (OR$_{Q4 vs Q1}$ = 2.20, 95% CI = 1.20 to 4.03; P_{trend} = .01) were independently and strongly predictive of increased breast cancer risk. In combination, women with high epithelium-to-stroma proportion and high MBD had substantially higher risk than those with low epithelium-to-stroma proportion and low MBD (OR = 2.27, 95% CI = 1.27 to 4.06; P_{trend} = .005), particularly among women with nonproliferative (P_{trend} = .01) vs proliferative (P_{trend} = .33) BBD.
Conclusion: Among BBD patients, increasing epithelium-to-stroma proportion on BBD biopsies and percent MBD at BBD diagnosis were independently and jointly associated with increasing breast cancer risk. These findings were particularly striking for women with nonproliferative disease (comprising approximately 70% of all BBD patients), for whom relevant predictive biomarkers are lacking.

In the United States, more than 70% of 1.6 million annual breast biopsies are benign (1,2). Although one of the strongest breast cancer risk factors (3,4), not all women with benign breast disease (BBD) will develop breast cancer. To date, conventional approaches for risk stratification in BBD patients rely on microscopic assessment of epithelial abnormalities on BBD biopsies to classify women as having nonproliferative disease or proliferative disease without or with atypia (4-6). Patients with nonproliferative disease (approximately 70% of all BBD patients) are at minimal or no increased breast cancer risk (5).

Proliferative diseases comprise approximately 30% of all BBD biopsies, and these patients have an almost 2-fold increased risk of breast cancer, with even higher 4-fold increased risk in the presence of atypical hyperplasia (7). Notably, atypical hyperplasia diagnoses comprise only approximately 4% of all BBD patients, and in absolute terms, fewer breast cancers will occur in these women than in those with nonproliferative BBD (8). Thus, there is the need to uncover additional tissue biomarkers that can aid to further stratify BBD patients into different breast cancer risk categories.

Microscopically, the normal breast is comprised of epithelial, stromal, and adipose tissue components (9). Although qualitative aberrations in epithelium underpin BBD-related breast cancer risk (10), the role of quantitative variation is poorly understood. Moreover, it remains fundamentally unclear whether risks related to BBD are driven by aberrations in the epithelium alone or via a dynamic interplay involving the stroma (11). Women undergoing breast biopsy, and for whom concomitant mammograms are available, represent an important patient population for the integrated study of histologic and radiologic breast tissue composition metrics in relation to breast cancer risk.

Within a cohort of women diagnosed as having BBD within a general community health-care plan, we leveraged supervised machine-learning (12) and computer-assisted thresholding (13) methods to quantify breast tissue composition on histological and radiological images, respectively. This approach facilitated our investigations of the independent and joint associations of quantitative tissue metrics present at the time of BBD diagnosis with risk of subsequent breast cancer development.

Methods

Study Population and Design

We conducted a nested case-control study within a cohort of 15 395 women aged 18-86 years who were biopsied for BBD within the Kaiser Permanente Northwest Region (KPNW) between 1970 and 2012, with follow-up through mid-2015. KPNW is a prepaid health-care plan with more than 500 000 members with facilities in Washington and Oregon. About 82% of KPNW members are White, 5% Asian American, 5% Hispanic, 3% African American, and 5% other ethnicities (14). Case-control definition, ascertainment, and selection have been described in detail (15). Cases were women with a BBD biopsy who subsequently developed invasive breast cancer 1 year or more after the index BBD biopsy. Controls were women biopsied for BBD at the same time as the cases who were alive but had not developed breast cancer during the same follow-up period as the corresponding cases. Controls were selected using risk-set sampling and were individually matched to corresponding cases on age at BBD diagnosis (+/- 1 year) and plan membership duration. Data on breast cancer risk factors around the time of BBD diagnosis were manually abstracted from medical records (15). The study was approved by the Committee on Clinical Investigations of the Albert Einstein College of Medicine, the Kaiser Permanente Northwest Biospecimen review committee, and the National Institutes of Health Office of Human Subjects Research.

Tissue Block Retrieval and Analysis of Digitized Hematoxylin and Eosin (H&E)–Stained Sections

The most representative formalin-fixed paraffin-embedded tissue block on which the final clinical diagnosis of BBD was based was retrieved for each patient and H&E-stained cut sections were prepared. BBD lesions on H&E-stained slides were subsequently classified according to Dupont and Page criteria as normal or nonproliferative, proliferative without atypia, and atypical hyperplasia (3). Terminal duct lobular unit (TDLU) involution was visually assessed based on published criteria from the Mayo BBD cohort (16) as follows: none (<25% of TDLUs involuted), partial (25%-74%), or complete (≥75%) involution.

H&E-stained slides were scanned at high resolution (20×) using the Aperio digital slide scanner (Leica Biosystems Inc, Buffalo Grove, IL). Of the 1028 slides, 50 were unscannable because of quality control issues. A 22-datapoint script involving 2 randomly selected representative images was trained by a pathologist (MA) with expertise in digital pathology to identify, segment, and quantify (in mm^2) areas on each slide comprised of epithelium (6-datapoints), stroma (5-datapoints), and adipose tissue (11-datapoints) as shown in Figure 1. Training and centralized image analysis were performed masked to all patient characteristics. In reproducibility analysis, another pathologist (MAD) independently developed a 37-datapoint script to analyze a random sample of 185 (approximately 20%) images. The results showed excellent agreement between the 2 pathologists' scripts (Spearman rho = 0.95, 0.97, and 0.98 for epithelium, stroma, and adipose tissue areas, respectively; Supplementary Table 1, available online).

Percent epithelium, stroma, and adipose tissue were calculated by dividing the absolute value of each histologic metric by total tissue area on the slide and multiplying by 100. Given the documented biologic relevance of tumor-stroma ratio in the setting of cancer progression (17,18), we sought to evaluate an equivalent feature in the context of BBD progression. Accordingly, we calculated the proportion of fibroglandular tissue (ie, epithelium plus stroma) on histology slides that was epithelium relative to stroma, that is, histologic epithelium-to-stroma proportion (histologic-ESP), by dividing epithelial area by total fibroglandular tissue area and multiplying by 100.

Mammogram Retrieval and Mammographic Breast Density Assessment

The most recent mammograms occurring approximately 6 months before (preferably) or up to 1 month after the BBD biopsy were retrieved. Craniocaudal film mammographic views of the ipsilateral (preferable; 89%) or contralateral (11%) breast were digitized using an Array Corporation 2095 Laser Film Digitizer (Roden, the Netherlands; optical density = 4.0). Prior studies have demonstrated high within-woman concordance for density measures and have found mammographic density (MBD) to be predictive of risk irrespective of laterality (19). Quantitative measures of density were obtained using Cumulus, an interactive computer-assisted thresholding program (20), with demonstrated validity with respect to breast cancer risk associations in numerous epidemiologic studies (21). All mammograms were evaluated by a single expert reader (EAB), who measured absolute dense area (cm^2) and total breast area (cm^2) as described previously (20). Percentage MBD was calculated by dividing the dense breast area by the total breast area and multiplying by 100 (see Figure 1). Images from cases
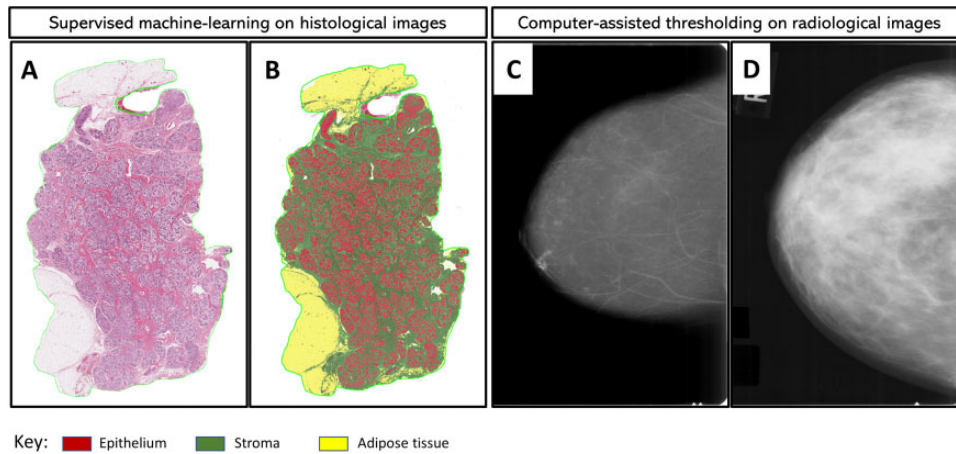
Figure 1. Quantitative assessment of breast tissue composition metrics from digitized histological and radiological images. Supervised machine-learning and computer-assisted thresholding methods were applied to histologic **(A and B)** and radiologic **(C and D)** images from women with benign breast disease (BBD), respectively. Diagnostic hematoxylin and eosin (H&E)–stained slides were digitized for image analysis, and mammograms performed around the time of BBD diagnosis (average 1.3 months) were retrieved and digitized for analysis. H&E image analysis was performed using the commercially available Halo version 1.2 Tissue Classifier algorithm (Indica Labs, Albuquerque, NM), which is a random forest algorithm that is specifically designed for the identification and classification of tissue types based on color, texture, and other contextual features. For training purposes, a representative H&E image was randomly selected, and the machine was trained to identify areas of epithelium **(red)**, stroma **(green)**, and adipose tissue **(yellow)**. **Panel A** is an example of an H&E image before analysis. In **panel B**, the machine learns by example to accurately classify and quantify epithelial **(red)**, stromal **(green)**, and adipose tissue **(yellow)** areas. **Panels C and D** are examples of representative mammograms that were determined to have low (below the median distribution among controls) and high (above the median) percent mammographic breast density based on quantitative assessment using the Cumulus software interface.

and matched controls were assessed within the same batch and in random order. A repeat set of 113 images was assessed for reliability. The intraclass correlation coefficients for percent MBD, dense area, and total breast area were 0.92, 0.89, and 0.99, respectively, documenting excellent reproducibility.

Statistical Analysis

Associations between baseline patient characteristics and tissue composition metrics were assessed in multivariable linear regression models fitted to controls. Locally weighted scatter plots of log residuals after regressing body mass index and histology were used to demonstrate the distributions of tissue composition metrics by age among cases and controls. Quartiles (Q1-Q4) of tissue composition metrics were defined based on their distributions among controls. Associations between tissue composition metrics and breast cancer risk were assessed in crude and adjusted logistic regression models. For histologic metrics, conditional logistic regression models were adjusted for age at menarche, parity and age at first live birth, body mass index, menopausal status and menopausal hormone therapy use, bilateral oophorectomy, history of breast cancer in a first-degree relative, BBD histology, extent of lobular involution, and calendar year of BBD diagnosis, as well as MBD. We used a likelihood ratio (LR) test to compare fit of a fully adjusted model with epithelium to one with histologic-ESP. Because radiologic tissue metrics were less complete for cases and controls, we used unconditional logistic regression, adjusting for matching factors (age at BBD diagnosis and follow-up duration), other risk factors noted above, as well as histologic-ESP, which showed better model fit than epithelium. To test the joint effects of histologic-ESP and MBD, both variables were dichotomized based on their median values among controls, and a composite variable combining both was defined. Missing covariate values (Supplementary Table 2, available online) were imputed using the multiple (×5) imputation by chained equations

approach (22) with appropriate variance adjustment by Rubin's formula (23) for all analyses. All analyses were performed overall and stratified by BBD histological classification. P_{trend} was estimated by including quartiles of tissue composition metrics as continuous variables in multivariable models. P values for heterogeneity were obtained by including multiplicative interaction terms between BBD histology and relevant risk factors in the full model. All analyses were 2-sided and were performed using Stata statistical software version 16.1. A P value of less than .05 was considered statistically significant.

Results

Characteristics of BBD Patients at Baseline

A total of 514 cases and 514 controls (n = 1028 patients) with BBD were included in this study. Of these, more than 95% (488 controls, 486 cases) had an H&E suitable for digitized pathology assessment, with a single image failing analysis. For radiologic metrics, 302 (58.8%) controls and 296 (57.6%) cases had mammograms available within an average of 1.3 (SD = 3.5) months of BBD diagnosis. Most of the missing mammograms were for women diagnosed with BBD in the prescreening (<1985) era. For those with BBD diagnosed in 1985 or thereafter, more than 85.0% of cases and controls had available mammograms for MBD assessment. In total, 564 patients (284 controls and 280 cases) had data on both histologic and radiologic metrics (Supplementary Figure 1, available online). Baseline patient characteristics did not differ between those with available or missing histologic metrics (Supplementary Table 3, available online). For radiologic metrics, differences were mostly related to screening availability by calendar period (Supplementary Tables 3 and 4, available online). The median (range) age of patients at BBD diagnosis was 51.5 (18.7-86.6) years. BBD lesions were predominantly nonproliferative (68.9%), with fewer (27.9%) proliferative disease and atypical hyperplasia (3.2%). The distributions of other patient baseline characteristics are shown in Table 1.

Table 1. Baseline characteristics of the benign breast disease (BBD) patients, overall and by breast cancer case-control status, Kaiser Permanente Northwest Center for Health Research, 1970-2015

| Characteristic	Overall, No. (%) (n = 1028)	Controls, No. (%) (n = 514)	Cases, No. (%) (n = 514)	P[a]
Median age at BBD (range), y	51.5 (18.7-86.6)	51.4 (21.7-86.2)	51.5 (18.7-86.6)	.97
Median follow-up time (range), y	9 (0.6-37.5)	9 (0.6-37.3)	9 (1.0-37.5)	1.00
Age at menarche, y				
≤12	368 (45.5)	185 (44.6)	183 (46.4)	.62
13	245 (30.3)	132 (31.8)	113 (28.7)	
≥ 14	198 (24.2)	98 (23.6)	98 (24.9)	
Parity and age at first live birth				
Nulliparous/AFLB ≥30 y	225 (25.9)	98 (22.1)	127 (30.0)	.008
Parous/AFLB <30 y	643 (74.1)	346 (77.9)	297 (70.0)	
Body mass index, kg/m²				
<25	425 (45.8)	213 (45.8)	212 (45.7)	.72
25-30	281 (30.2)	136 (29.2)	145 (31.2)	
>30	223 (24.0)	116 (25.0)	107 (23.1)	
Family history				
Absent	791 (82.2)	408 (84.6)	383 (79.8)	.04
Present	171 (17.8)	74 (15.4)	97 (20.2)	
Menopause and MHT use				
Premenopausal	412 (43.4)	203 (41.9)	209 (45.0)	.12
Postmenopausal MHT use	393 (41.4)	211 (43.5)	182 (39.2)	
Postmenopausal no MHT	20 (2.1)	14 (2.9)	6 (1.3)	
Postmenopausal unknown MHT	124 (13.1)	57 (11.7)	67 (14.5)	
Bilateral oophorectomy				
No	805 (86.3)	394 (83.8)	411 (88.8)	.02
Yes	128 (13.7)	76 (16.2)	52 (11.2)	
BBD histology				
Nonproliferative	708 (68.9)	384 (74.7)	324 (63.0)	<.001
Proliferative, no atypia	287 (27.9)	124 (24.1)	163 (31.7)	
Atypical hyperplasia	33 (3.2)	6 (1.2)	27 (5.3)	
Sclerosing adenosis				
Absent	942 (91.6)	478 (93.0)	464 (90.3)	.11
Present	86 (8.4)	36 (7.0)	50 (9.7)	
Radial scar present				
Absent	977 (95.0)	497 (96.7)	480 (93.4)	.01
Present	51 (5.0)	17 (3.3)	34 (6.6)	
Fibroadenoma				
Absent	878 (85.4)	439 (85.4)	439 (85.4)	.74
Simple	133 (12.9)	68 (13.2)	65 (12.6)	
Complex	17 (1.7)	7 (1.4)	10 (2.0)	
Columnar cell hyperplasia				
Absent	875 (85.5)	450 (87.9)	425 (83.0)	.03
Present	149 (14.5)	62 (12.1)	87 (17.0)	
Lobular involution				
Absent	475 (52.5)	235 (52.8)	240 (52.2)	.09
Partial	176 (19.5)	75 (16.9)	101 (22.0)	
Complete	254 (28.0)	135 (30.3)	119 (25.8)	

[a]P values comparing cases and controls were obtained from χ^2 tests (for categorical variables) and Kruskal-Wallis test (for continuous variables). AFLB = age at first live birth; MHT = menopausal hormone therapy use.

Tissue Composition Metrics in Relation to Patients' Baseline Characteristics

The median (range) of percent epithelial, stromal, adipose tissue and histologic-ESP distributions were 8.4% (0.2%-97.4%), 38.1% (1.3%-88.9%), 48.0% (1.3%-97.5%), and 19.9% (0.9%-98.6%), respectively. Medians (ranges) for absolute dense and nondense areas and percent MBD were 36.3 (0-232.2) cm², 96.4 (5.9-375.5) cm², and 30.2% (0.0%-86.9%), respectively (Supplementary Table 5, available online). The correlations between histologic and radiologic tissue composition metrics and their associations with baseline patient characteristics are provided in Supplementary Tables 6 and 7 (available online, respectively).

As shown in Figure 2, the fat component of the breast was higher in older than younger women at the time of BBD diagnosis and among controls than cases across all age groups. In contrast, the fibroglandular tissue component was higher in younger than older women at BBD diagnosis and among cases than controls across all age groups. The amount of stroma did not differ between cases and controls aged younger than 60 years. Controls aged older than 60 years had higher stromal content than cases. Histologic-ESP was higher among cases than controls between ages 40 and 50 years and older than 60 years.
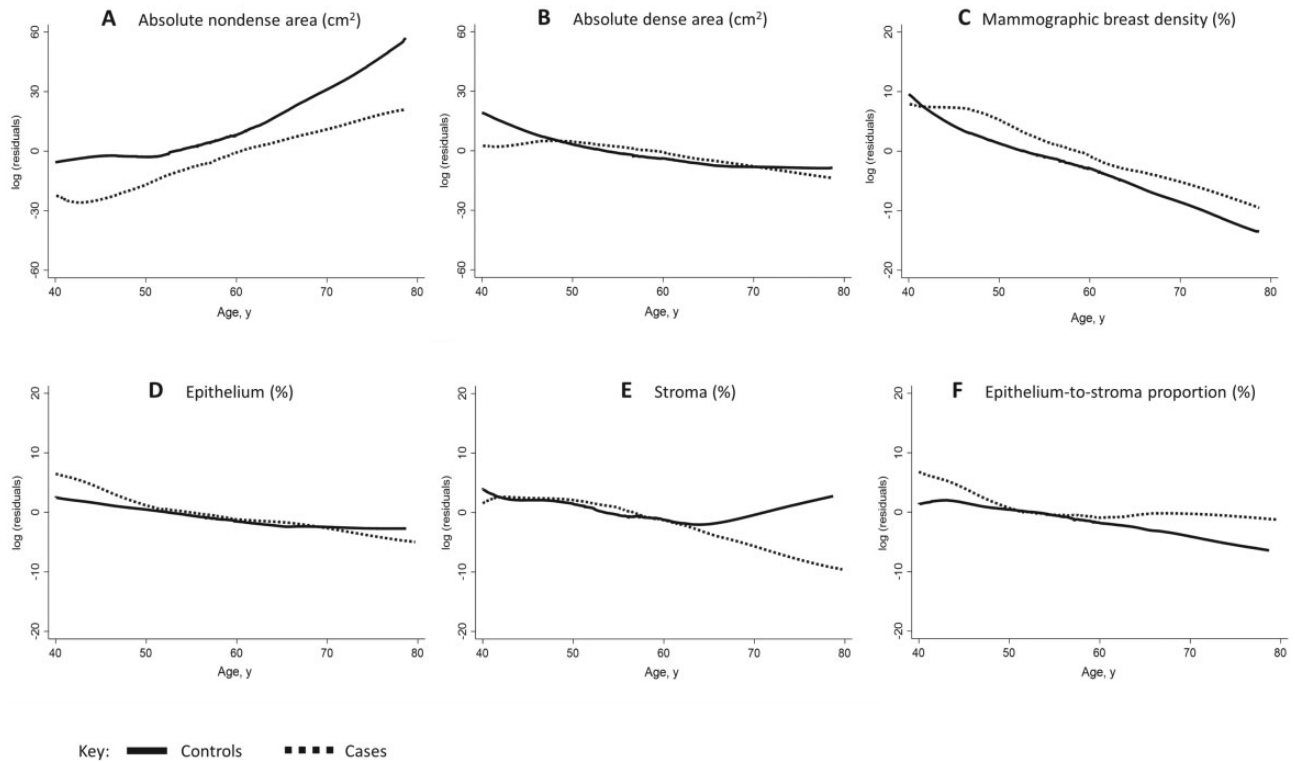
Figure 2. Histologic and radiologic breast tissue composition metrics by age and case-control status. Locally weighted scatter plot smoothing of log residuals (y-axes) from linear regression models of nondense area (**A**), dense area (**B**), percent mammographic breast density (**C**), epithelium (**D**), stroma (**E**), and epithelium-to-stroma proportion (**F**). The effects of body mass index and benign breast disease histology on breast tissue composition were accounted for by adjusting for these in the linear regression models and plotting the log residuals against age.

Associations Between Histologic Metrics and Breast Cancer Risk

The median (range) time between BBD diagnosis and breast cancer incidence was 9 (1.0-37.5) years. As shown in Table 2, increasing epithelial content on BBD biopsies was associated with increasing breast cancer risk (odds ratio [OR]$_{Q4\ vs\ Q1}$ = 1.85, 95% confidence interval [CI] = 1.13 to 3.04; P$_{trend}$ = .02), irrespective of BBD histology (P$_{heterogeneity}$ = .74). Conversely, the association between stroma and breast cancer risk differed by BBD histology (P$_{heterogeneity}$ = 0.002). Among women with nonproliferative disease, increasing stroma was associated with decreasing breast cancer risk (OR$_{Q4\ vs\ Q1}$ = 0.51, 95% CI = 0.32 to 0.81; P$_{trend}$ = .006), whereas among those with proliferative disease, it was associated with increasing risk (OR$_{Q4\ vs\ Q1}$ = 2.52, 95% CI = 1.00 to 6.32; P$_{trend}$ = .07). Histologic-ESP (LRχ^2 = 8.4; P = .03) provided a better model fit than epithelium (LRχ^2 = 7.4; P = .06) and was associated with statistically significant increased risk of breast cancer (OR$_{Q4\ vs\ Q1}$ = 2.06, 95% CI = 1.28, 3.33; P$_{trend}$ = .002), irrespective of BBD histology (P$_{heterogeneity}$ = .52). Histologic-ESP remained associated with breast cancer risk (OR$_{Q4vsQ1}$ = 2.10, 95% CI = 1.33 to 3.32; P$_{trend}$ = .002) even after adjusting for specific BBD histologic features.

Associations Between Radiologic Metrics and Breast Cancer Risk

As shown in Table 3, increasing percent MBD was associated with increasing risk of breast cancer (OR$_{Q4\ vs\ Q1}$ = 2.20, 95% CI = 1.20 to 4.03; P$_{trend}$ = .01), irrespective of BBD histology (P$_{heterogeneity}$ = .75).

Joint Associations of Histologic-ESP and MBD With Breast Cancer Risk

Following dichotomization at their median values among controls, high histologic-ESP and percent MBD remained statistically significantly associated with elevated breast cancer risk (OR = 1.57, 95% CI = 1.13 to 2.18, and OR = 1.50, 95% CI = 1.01 to 2.24, respectively) (Table 4). Further, patients with high histologic-ESP had higher breast cancer risk than those with low histologic-ESP, irrespective of whether they had high (OR = 2.06, 95% CI = 1.09 to 3.88) or low (OR = 1.60, 95% CI = 0.93 to 3.88) MBD (Figure 3). Breast cancer risk was substantially higher in women with combined high histologic-ESP and high MBD than in those with low histologic-ESP and low MBD (OR = 2.27, 95% CI = 1.27 to 4.06; P$_{trend}$ = .005). These findings were stronger in patients with nonproliferative (OR = 2.43, 95% CI = 1.20 to 4.93) vs proliferative (OR = 1.55, 95% CI = 0.45 to 5.33) disease, although statistically significant heterogeneity was not observed (P$_{heterogeneity}$ = .73).

In analysis evaluating the potential value of histologic-ESP and MBD in predicting subsequent breast cancer, we calculated area under the receiver operating characteristics curves (AUCs); we found AUCs of 0.587, 0.607, 0.610, and 0.624 for BBD histology alone; BBD histology and histologic-ESP; BBD histology and MBD; and BBD histology and histologic-ESP and MBD, respectively, suggesting incremental value for these metrics in predicting subsequent breast cancer.

In sensitivity analyses, histologic-ESP and percent MBD were associated with elevated breast cancer risk before and after multiple imputation and irrespective of menopausal status, BBD-to-tumor laterality, calendar period of BBD diagnosis, or

Table 2. Odds ratios (ORs) and 95% confidence intervals (CIs) for the associations between histologic tissue composition metrics and risk of subsequent breast cancer development among women with BBD, overall and by BBD histological classification[a]

Histologic tissue metrics[b]	Overall		Nonproliferative		Proliferative		P_{het}
	Controls/Cases	OR (95% CI)	Controls/Cases	OR (95% CI)	Controls/Cases	OR (95% CI)	
Epithelium area (%)							
Quartiles							
Q1 (<4.45)	122/103	1.00 (referent)	100/83	1.00 (referent)	22/20	1.00 (referent)	.74
Q2 (4.45-7.93)	122/111	1.10 (0.72 to 1.67)	100/78	1.02 (0.65 to 1.62)	22/33	1.30 (0.52 to 3.27)	
Q3 (7.93-14.36)	122/111	1.13 (0.72 to 1.76)	90/64	0.97 (0.59 to 1.57)	32/47	1.54 (0.64 to 3.74)	
Q4 (>14.36)	122/161	1.85 (1.13 to 3.04)	75/83	1.53 (0.93 to 2.54)	47/78	1.90 (0.81 to 4.47)	
P_{trend}		.02		.16		.15	
Per 10% increase	488/486	1.14 (0.99 to 1.29)	365/308	1.14 (0.98 to 1.29)	123/178	1.04 (0.86 to 1.22)	
P		.06		.08		.64	
Stroma area (%)							
Quartiles							
Q1 (<24.66)	122/134	1.00 (referent)	83/94	1.00 (referent)	39/40	1.00 (referent)	.002
Q2 (24.66-38.08)	122/107	0.62 (0.40 to 0.95)	85/59	0.48 (0.29 to 0.79)	37/48	1.09 (0.52 to 2.27)	
Q3 (38.08-53.70)	122/124	0.67 (0.43 to 1.05)	87/68	0.48 (0.29 to 0.79)	35/56	1.23 (0.61 to 2.51)	
Q4 (>53.70)	122/121	0.71 (0.46 to 1.11)	110/87	0.51 (0.32 to 0.81)	12/34	2.52 (1.00 to 6.32)	
P_{trend}		.16		.006		.07	
Per 10% increase	488/486	0.96 (0.87 to 1.03)	365/308	0.88 (0.80 to 0.97)	123/178	1.17 (1.01 to 1.33)	
P		.24		.01		.03	
Adipose tissue area (%)							
Quartiles							
Q1 (<29.42)	122/135	1.00 (referent)	97/81	1.00 (referent)	25/54	1.00 (referent)	.03
Q2 (29.42-49.73)	122/132	0.99 (0.65 to 1.51)	89/74	1.03 (0.65 to 1.63)	33/58	0.86 (0.42 to 1.76)	
Q3 (49.73-66.58)	122/99	0.81 (0.54 to 1.21)	88/66	0.97 (0.61 to 1.55)	34/33	0.44 (0.20 to 0.96)	
Q4 (>66.58)	122/120	1.15 (0.73 to 1.81)	91/87	1.61 (0.98 to 2.64)	31/33	0.56 (0.23 to 1.34)	
P_{trend}		.88		.09		.06	
Per 10% increase	488/486	1.01 (0.95 to 1.08)	365/308	1.06 (0.99 to 1.14)	123/178	0.93 (0.80 to 1.06)	
P		.69		.09		.30	
Histologic-ESP (%)							
Quartiles							
Q1 (<10.82)	122/93	1.00 (referent)	109/77	1.00 (referent)	13/16	1.00 (referent)	.52
Q2 (10.82-18.23)	122/110	1.24 (0.82 to 1.88)	99/79	1.20 (0.78 to 1.87)	23/31	1.08 (0.39 to 2.95)	
Q3 (18.24-29.01)	122/131	1.58 (1.02 to 2.45)	85/72	1.40 (0.89 to 2.23)	37/59	1.41 (0.54 to 3.66)	
Q4 (>29.01)	122/152	2.06 (1.28 to 3.33)	72/80	1.95 (1.21 to 3.16)	50/72	1.46 (0.57 to 3.71)	
P_{trend}		.002		.006		.32	
Per 10% increase	488/486	1.15 (1.04 to 1.27)	365/308	1.17 (1.06 to 1.30)	123/178	1.00 (0.85 to 1.15)	
P		.01		.004		.97	

[a]Benign breast disease (BBD) was classified as normal or nonproliferative and proliferative (with or without atypia). P_{het} = P value for heterogeneity of OR estimates by BBD histological classification.
[b]Quartiles (Q1-Q4) of percent histologic tissue composition metrics (epithelium, stroma, adipose tissue, histologic epithelium-to-stroma proportion [histologic-ESP]) were defined based on their distributions among controls. In overall analyses, multivariate conditional logistic regression models adjusted for age at menarche, parity and age at first live birth, body mass index, menopausal status and menopausal hormone therapy use, bilateral oophorectomy, history of breast cancer in a first-degree relative, BBD histology, extent of lobular involution, and calendar year of BBD diagnosis, as well as mammographic density, were used to estimate odds ratios and corresponding 95% confidence intervals. In stratified analyses by BBD histology (ie, nonproliferative disease and proliferative disease, with or without atypia), unconditional logistic regression models additionally adjusted for matching factors (ie, age at BBD diagnosis and follow-up time) were used to estimate odds ratios and 95% confidence intervals. Epithelium and stroma were mutually adjusted for one another, and histologic-ESP was additionally adjusted for adipose tissue.

time from BBD diagnosis to cancer development. Although histologic-ESP more strongly predisposed to estrogen receptor (ER)–positive ($OR_{Q4\ vs\ Q1}$ = 1.71, 95% CI = 1.10 to 2.68; P_{trend} =.009) than ER-negative ($OR_{Q4\ vs\ Q1}$ = 1.19, 95% CI = 0.50 to 2.80; P_{trend} =.39), as well as high-grade ($OR_{Q4\ vs\ Q1}$ = 2.08, 95% CI = 1.25 to 3.44; P_{trend} =.002) than low-grade ($OR_{Q4\ vs\ Q1}$ = 1.25, 95% CI = 0.65 to 2.39; P_{trend} =.41) tumors, differences by these tumor characteristics were not statistically significant.

Discussion

To our knowledge, this is the first study to combine machine-learning and computer-assisted thresholding methods in the setting of BBD for histologic and radiologic assessments of tissue composition metrics, respectively, and to simultaneously relate these to breast cancer risk. We found statistically significant relationships of histologic-ESP, a metric of the proportion of fibroglandular tissue on breast biopsies that is epithelium relative to stroma, and percent MBD, a metric of the proportion of total tissue area on mammograms that is radiodense, with risk of breast cancer development. Histologic-ESP and percent MBD were independently associated with risk; women with combined high histologic-ESP and high MBD had substantially higher breast cancer risk than those with low histologic-ESP and low MBD. The association between increasing stroma and breast cancer risk varied by the extent of epithelial hyperplasia; increasing stroma was associated with reduced risk in women

Table 3. Odds ratios (ORs) and 95% confidence intervals (CIs) for the associations between radiologic tissue composition metrics and risk of subsequent breast cancer development among women with BBD, overall and by BBD histological classification[a]

Radiologic tissue metrics[b]	Overall		Nonproliferative		Proliferative		
	Controls/Cases	OR (95% CI)	Controls/Cases	OR (95% CI)	Controls/Cases	OR (95% CI)	P_{het}
Absolute dense area (cm^2)							
Quartiles							
Q1 (<21.87)	76/59	1.00 (referent)	54/36	1.00 (referent)	22/23	1.00 (referent)	.84
Q2 (21.87-35.54)	75/79	1.21 (0.71 to 2.06)	54/41	0.99 (0.52 to 1.91)	21/38	2.05 (0.79 to 5.34)	
Q3 (35.54-58.94)	75/89	1.28 (0.75 to 2.17)	50/49	1.34 (0.69 to 2.59)	25/40	1.16 (0.45 to 2.98)	
Q4 (>58.94)	76/69	1.14 (0.66 to 1.95)	59/42	1.09 (0.57 to 2.09)	17/27	1.23 (0.41 to 3.67)	
P_{trend}		.50		.46		.99	
Per 10 cm^2 increase	302/296	1.02 (0.96 to 1.07)	217/168	1.02 (0.95 to 1.09)	85/128	1.00 (0.88 to 1.12)	
P		.58		.61		.95	
Absolute nondense area (cm^2)							
Quartiles							
Q1 (<59.98)	75/86	1.00 (referent)	56/48	1.00 (referent)	19/38	1.00 (referent)	.22
Q2 (59.98-101.24)	76/79	0.88 (0.53 to 1.46)	54/43	0.94 (0.51 to 1.73)	22/36	0.76 (0.27 to 2.12)	
Q3 (101.24-164.69)	75/99	0.97 (0.56 to 1.68)	53/55	1.12 (0.56 to 2.22)	22/44	0.67 (0.21 to 2.12)	
Q4 (>164.69)	76/32	0.27 (0.13 to 0.54)	54/22	0.40 (0.17 to 0.92)	22/10	0.11 (0.02 to 0.54)	
P_{trend}		.002		.08		.01	
Per 10 cm^2 increase	302/296	0.95 (0.92 to 0.99)	217/168	0.97 (0.94 to 1.01)	85/128	0.88 (0.79 to 0.96)	
P		.005		.17		.006	
Mammographic density (%)							
Quartiles							
Q1 (<14.67)	75/49	1.00 (referent)	53/31	1.00 (referent)	22/18	1.00 (referent)	.75
Q2 (14.67-28.39)	76/78	1.58 (0.94 to 2.68)	50/39	1.48 (0.77 to 2.86)	26/39	1.69 (0.66 to 4.34)	
Q3 (28.39-43.76)	76/82	1.88 (1.10 to 3.24)	61/45	1.52 (0.79 to 2.93)	15/37	3.26 (1.14 to 9.26)	
Q4 (>43.76)	75/87	2.20 (1.20 to 4.03)	53/53	2.29 (1.09 to 4.83)	22/34	1.81 (0.56 to 5.93)	
P_{trend}		.01		.04		.21	
Per 10% increase	302/296	1.12 (1.01 to 1.23)	217/168	1.10 (0.96 to 1.23)	85/128	1.15 (0.94 to 1.37)	
P		.03		.15		.16	

[a]Benign breast disease (BBD) was classified as normal or nonproliferative and proliferative (with or without atypia). P_{het} = P value for heterogeneity of OR estimates by BBD histological classification.

[b]Quartiles (Q1-Q4) of radiologic tissue composition metrics (absolute dense area [cm^2], absolute nondense area [cm^2], percent mammographic breast density [MBD] [%]) were defined based on their distributions among controls. Overall and in women with nonproliferative or proliferative disease (with or without atypia), unconditional logistic regression models were adjusted for age at menarche, parity and age at first live birth, body mass index, menopausal status and menopausal hormone therapy (MHT) use, bilateral oophorectomy, history of breast cancer in a first-degree relative, BBD histology, extent of lobular involution, calendar year of BBD diagnosis, and matching factors (age at BBD diagnosis and follow-up time from BBD to cancer), as well as histologic-ESP. Dense and nondense areas were mutually adjusted for one another.

with nonproliferative disease and increased risk in those with proliferative disease. This finding has not been reported previously and suggests a possible dual role of the stroma in mediating progression of breast precursor lesions. These results were robust to adjustments for other breast cancer risk factors. Taken together, our findings provide new insights into breast cancer development following BBD and could have implications for improved risk stratification and the clinical management of women with BBD, particularly those with nonproliferative disease, a large group for whom relevant predictive biomarkers are lacking.

To date, apart from BBD histological classification, very few risk factors for breast cancer have been identified for women with BBD. A few studies have reported the potential value of immunohistochemical markers, including ER and/or progesterone receptor expression, Ki-67, and CD20, in predicting risk, but these have yet to be consistently validated (24-27). Other reports support the value of TDLU involution in predicting breast cancer development following BBD (16,28-30). However, these studies have largely been based on qualitative assessments of involution, with limited stratification. Although standardized measures of involution have been proposed (30), these are difficult to obtain and rely on the availability of "normal," nonlesional tissue regions on BBD biopsies. Our findings of independent relationships of histologic-ESP and percent MBD with increasing breast cancer risk demonstrate the potential for these quantitative markers to improve risk stratification for BBD patients. Notably, histologic-ESP is a tissue-based feature that can easily be assessed on the same H&E slides used for BBD diagnosis, without requiring immunohistochemical or other special stains. Accordingly, measures of histologic-ESP on BBD diagnostic H&E slides can be combined with MBD around the time of BBD diagnosis to provide additional information to women regarding their future breast cancer risk, at minimal or no extra cost or effort.

Despite experimental evidence to support a context-dependent role of stroma to either prevent or promote carcinogenesis (31-36), the precise sequence and timing of events leading to a switch in stromal function from anti- to protumorigenesis remains poorly understood. The prevailing model for BBD progression to cancer is that of a sequence of worsening epithelial abnormalities from normal or

Table 4. Odds ratios (ORs) and 95% confidence intervals (CIs) for the joint associations of epithelium-to-stroma proportion and percent MBD in relation to breast cancer risk among women with BBD, overall and by BBD histological classification[a]

	Overall		Nonproliferative		Proliferative	
Characteristic	Controls/Cases	OR (95% CI)	Controls/Cases	OR (95% CI)	Controls/Cases	OR (95% CI)
Binary categories[b]						
Histologic-ESP						
Low	244/203	1.00 (referent)	208/156	1.00 (referent)	36/47	1.00 (referent)
High	244/283	1.57 (1.13 to 2.18)	157/152	1.50 (1.08 to 2.10)	87/131	1.37 (0.76 to 2.45)
P		.008		.01		.29
MBD						
Low	151/127	1.00 (referent)	208/156	1.00 (referent)	36/47	1.00 (referent)
High	151/169	1.50 (1.01 to 2.24)	157/152	1.45 (0.87 to 2.41)	87/131	1.73 (0.83 to 3.59)
P		.04		.15		.32
Joint associations						
Low histologic-ESP/low MBD	65/42	1.00 (referent)	57/32	1.00 (referent)	8/10	1.00 (referent)
Low histologic-ESP/high MBD	79/65	1.39 (0.78 to 2.48)	65/47	1.60 (0.81 to 3.13)	14/18	0.93 (0.24 to 3.54)
High histologic-ESP/low MBD	75/80	1.53 (0.88 to 2.67)	38/34	1.89 (0.95 to 3.76)	37/46	0.82 (0.26 to 2.63)
High histologic-ESP/high MBD	65/93	2.27 (1.27 to 4.06)	44/48	2.43 (1.20 to 4.93)	21/45	1.55 (0.45 to 5.33)
P_{trend}		.005		.01		.33

[a]Benign breast disease (BBD) was classified as normal or nonproliferative and proliferative (with or without atypia).
[b]Binary categories of histologic epithelium-stroma proportion (histologic-ESP) and mammographic density (MBD) were defined based on the median values among controls (ie, 18.2% and 28.4%, respectively). Models were adjusted for BBD histology, lobular involution, menopause and menopausal hormone therapy use, history of bilateral oophorectomy, parity and age at first full term live birth, age at menarche, family history of breast cancer in a first-degree relative, body mass index, MBD (for histologic-ESP), histologic-ESP (for MBD), calendar period of BBD diagnosis, and matching factors (ie, age at BBD diagnosis, follow-up time).
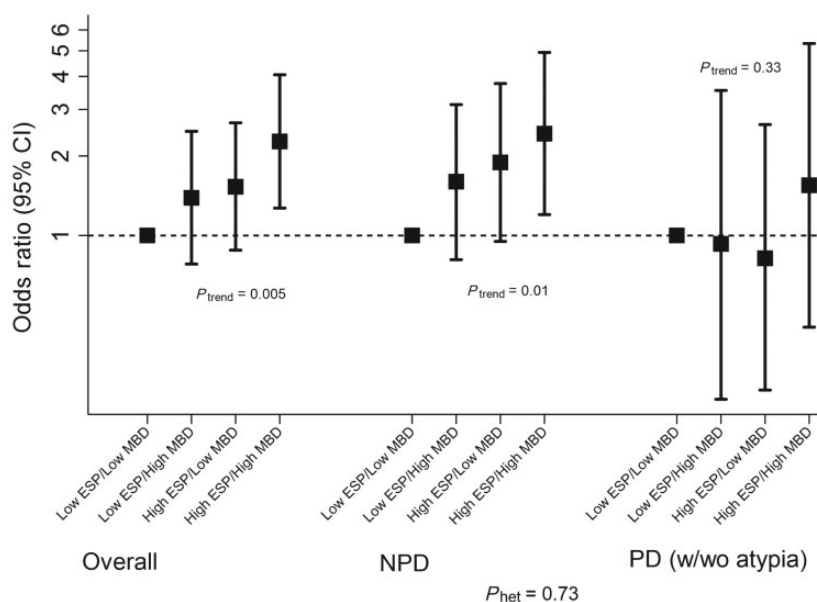

Figure 3. Joint associations of histologic epithelium-to-stroma proportion (histologic-ESP) and mammographic breast density (MBD) and risk of subsequent breast cancer development among women with benign breast disease (BBD). Histologic-ESP and percent MBD were dichotomized at their median values among controls (ie, 18.2% and 28.4%, respectively). Unconditional logistic regression models were adjusted for age at menarche, parity and age at first live birth, body mass index, menopausal status and menopausal hormone therapy use, history of breast cancer in a first-degree relative, BBD histology, extent of lobular involution, and calendar year of BBD diagnosis, as well as matching factors (age at BBD diagnosis and follow-up time from BBD to cancer). Analyses were performed overall (controls/cases, n = 284/280) and among BBD patients with nonproliferative disease (NPD; controls/cases, n = 204/161) and **(C)** proliferative disease (PD; with (w)/without(wo) atypia); controls/cases, n = 80/119). Detailed odds ratios and related estimates are presented in Table 4. P values for trend (P_{trend}) were assessed by modeling the joint ESP-MBD variable as continuous in the multivariable model. P value for heterogeneity (P_{het}) was obtained by including a multiplicative interaction term between the joint ESP-MBD variable and BBD histology in the overall, fully adjusted, model. All tests were 2-sided. CI = confidence interval.

nonproliferative to proliferative disease (without atypia), atypical hyperplasia, in situ carcinoma, and, ultimately, invasive breast cancer (37). Alternative pathways leading directly from normal or nonproliferative disease to invasive carcinoma have long been suspected (37), but specific tissue culprits are yet to be identified. Our finding of increasing breast cancer risk with

increasing histologic-ESP that was particularly strong in women with normal or nonproliferative BBD supports an alternative model involving aberrations in both epithelial and stromal compartments that favor carcinogenesis (Figure 4). In our proposed model, the transition from normal or nonproliferative to proliferative BBD is characterized by the loss of stromal protective
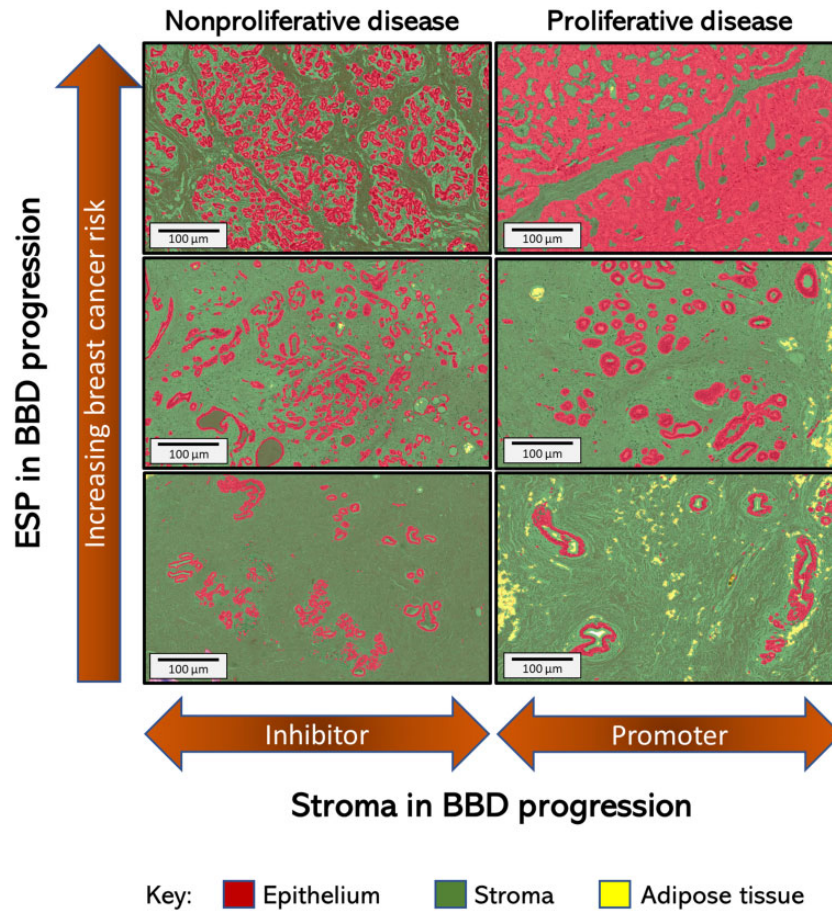
Figure 4. Conceptual model of benign breast disease (BBD) to breast cancer progression incorporating the contributions of histologic changes in epithelium, stroma, and epithelium-to-stroma proportion (ESP) to breast cancer risk. Increasing ESP is displayed vertically, from bottom to top, to correspond to observed association with increasing risk of subsequent breast cancer development in this study (Table 2). The context-dependent role of the stroma to either inhibit or promote tumor formation in the setting of nonproliferative or proliferative disease (Table 2), respectively, is displayed horizontally. In this conceptual model of BBD to breast cancer progression, we propose that the proportion of the epithelial and stromal components of the breast is in a delicate balance during normal homeostasis. Disruption of this balance, either through uncontrolled epithelial proliferation arising from endogenous and/or exogenous factors, lack of age-related epithelial involution, or via exogenous and/or endogenous causes of stromal depletion, will manifest as increasing histologic-ESP (Supplementary Table 7, available online). High histologic-ESP may, in turn, represent a feature of the breast microenvironment that is conducive to carcinogenesis.

effect as well as by a "proliferative-switch" in stromal function from tumor suppressor to tumor promoter.

An important aspect in the clinical management of women with BBD or high MBD is to decide who is at sufficiently high risk to benefit from preventative strategies, such as chemoprevention, that reduce risk of developing cancer. Available risk prediction tools (38-43) have modest discriminatory accuracy, which could be improved by adding quantitative tissue composition metrics such as histologic-ESP and percent MBD. Furthermore, more than 43% of screened US women have dense breasts (44), therefore, it is imperative to identify additional factors that may identify those at high risk of invasive disease, requiring further clinical management (45,46). In the current study, high histologic-ESP portended elevated breast cancer risk for women with low or high MBD, buttressing the importance of integrating histologic measures, when available, for distinguishing relative proportions of epithelium and stroma in radio-dense tissue, a distinction that cannot currently be made on mammograms.

Our application of machine-learning to digitized H&E slides allowed us to perform centralized analysis of all images using a single script, thereby limiting subject-specific bias and random error. The correlation between different scripts that were independently trained by 2 pathologists was excellent. This study, however, is not without limitations: most patients in this analysis underwent excisional biopsies, which have been largely replaced by needle biopsies as the standard of care. Also, there were too few women with atypical hyperplasia to allow for separate analysis. A primary goal of this analysis was to examine interrelationships between radiologic and histologic metrics with risk among BBD patients, and we did not have sufficient sample size to further refine MBD cut points beyond the median value, which may have led to underestimation of risk estimates. Future work involving larger samples sizes that also integrate more contemporary approaches, including artificial intelligence (47), for density assessment on digital mammography will be important for extending the present findings.

In summary, quantitative assessments of histologic-ESP on diagnostic BBD biopsy slides and percent MBD on mammograms performed around the time of BBD diagnosis were associated with increasing risk of subsequent invasive breast cancer development, particularly for women with nonproliferative disease. Furthermore, histologic-ESP identified women with low MBD who were at elevated risk of breast cancer and those with

high MBD who were not. We also uncovered a context-dependent role of the stroma to either decrease or increase breast cancer risk in women with nonproliferative vs proliferative disease, respectively. Taken together, these findings provide clues regarding breast cancer etiology and BBD progression and could have important implications for risk stratification and the clinical management of women with benign findings upon breast biopsy.

Funding

Notes

Role of the funders: The funders had no role in the design of the study; the collection, analysis, and interpretation of the data; the writing of the manuscript; and the decision to submit the manuscript for publication.

Disclosures: The authors declare no conflicts of interest.

Author contributions: Conception and design: MA, AGG, JDF, TER, GLG. Provision of study materials or patients: KR, AGG, TMK, TER. Generation, collection, and assembly of data: MA, SF, EAB, LW, MAD, RMP, RTF, SL, KR, AGG, TMK, TER. Data analysis and interpretation: All authors. Administrative support: RTF, SL, TMK. Manuscript writing: MA, SF, MAD, RMP, JDF, GLG. Final approval of manuscript: All authors.

Acknowledgements: We thank Dr Yihong Wang who performed the BBD pathology evaluations.

Data Availability

The authors will make the data available upon reasonable request and with permission of the Kaiser Permanente Center for Health Research in Portland, Oregon.

References

1. Silverstein M. Where's the outrage? *J Am Coll Surg*. 2009;208(1):78–79.
2. Gutwein LG, Ang DN, Liu H, et al. Utilization of minimally invasive breast biopsy for the evaluation of suspicious breast lesions. *Am J Surg*. 2011;202(2): 127–132.
3. Dupont WD, Page DL. Risk factors for breast cancer in women with proliferative breast disease. *N Engl J Med*. 1985;312(3):146–151.
4. Hartmann LC, Sellers TA, Frost MH, et al. Benign breast disease and the risk of breast cancer. *N Engl J Med*. 2005;353(3):229–237.
5. Santen RJ, Mansel R. Benign breast disorders. *N Engl J Med*. 2005;353(3): 275–285.
6. Hartmann LC, Degnim AC, Santen RJ, Dupont WD, Ghosh K. Atypical hyperplasia of the breast—risk assessment and management options. *N Engl J Med*. 2015;372(1):78–89.
7. Degnim AC, Dupont WD, Radisky DC, et al. Extent of atypical hyperplasia stratifies breast cancer risk in 2 independent cohorts of women. *Cancer*. 2016; 122(19):2971–2978.
8. Guray M, Sahin AA. Benign breast diseases: classification, diagnosis, and management. *Oncologist*. 2006;11(5):435–449.
9. Vorrherr H. *The Breast: Morphology, Physiology, and Lactation*. New York, NY: NY Academic Press; 1974.
10. Dupont WD, Parl FF, Hartmann WH, et al. Breast cancer risk associated with proliferative breast disease and atypical hyperplasia. *Cancer*. 1993;71(4): 1258–1265.
11. Wiseman BS, Werb Z. Stromal effects on mammary gland development and breast cancer. *Science*. 2002;296(5570):1046–1049.
12. Gurcan MN, Boucheron LE, Can A, Madabhushi A, Rajpoot NM, Yener B. Histopathological image analysis: a review. *IEEE Rev Biomed Eng*. 2009;2: 147–171.
13. Boyd NF, Byng JW, Jong RA, et al. Quantitative classification of mammographic densities and breast cancer risk: results from the Canadian National Breast Screening Study. *J Natl Cancer Inst*. 1995;87(9):670–675.
14. Glass AG, Lacey JV, Carreon JD, Hoover RN. Breast cancer incidence, 1980-2006: combined roles of menopausal hormone therapy, screening mammography, and estrogen receptor status. *J Natl Cancer Inst*. 2007;99(15):1152–1161.
15. Arthur R, Wang Y, Ye K, et al. Association between lifestyle, menstrual/reproductive history, and histological factors and risk of breast cancer in women biopsied for benign breast disease. *Breast Cancer Res Treat*. 2017;165(3): 623–631.
16. Milanese TR, Hartmann LC, Sellers TA, et al. Age-related lobular involution and risk of breast cancer. *J Natl Cancer Inst*. 2006;98(22):1600–1607.
17. Huijbers A, Tollenaar RAEM, V Pelt GW, et al. The proportion of tumor-stroma as a strong prognosticator for stage II and III colon cancer patients: validation in the VICTOR trial. *Ann Oncol*. 2013;24(1):179–185.
18. Downey CL, Simpkins SA, White J, et al. The prognostic significance of tumour-stroma ratio in oestrogen receptor-positive breast cancer. *Br J Cancer*. 2014;110(7):1744–1747.
19. Vachon CM, Brandt KR, Ghosh K, et al. Mammographic breast density as a general marker of breast cancer risk. *Cancer Epidemiol Biomarkers Prev*. 2007; 16(1):43–49.
20. Byng JW, Boyd NF, Fishell E, Jong RA, Yaffe MJ. The quantitative analysis of mammographic densities. *Phys Med Biol*. 1994;39(10):1629–1638.
21. McCormack VA, dos S, Silva I. Breast density and parenchymal patterns as markers of breast cancer risk: a meta-analysis. *Cancer Epidemiol Biomarkers Prev*. 2006;15(6):1159–1169.
22. White IR, Royston P, Wood AM. Multiple imputation using chained equations: issues and guidance for practice. *Stat Med*. 2011;30(4):377–399.
23. Rubin DB. *Multiple Imputation for Nonresponse in Surveys*. New York: John Wiley and Sons; 1987.
24. Huh SJ, Oh H, Peterson MA, et al. The proliferative activity of mammary epithelial cells in normal tissue predicts breast cancer risk in premenopausal women. *Cancer Res*. 2016;76(7):1926–1934.
25. Oh H, Eliassen AH, Wang M, et al. Expression of estrogen receptor, progesterone receptor, and Ki67 in normal breast tissue in relation to subsequent risk of breast cancer. *NPJ Breast Cancer*. 2016;2(1):16032.
26. Posso M, Corominas JM, Serrano L, et al.; the BELE Study Group. Biomarkers expression in benign breast diseases and risk of subsequent breast cancer: a case-control study. *Cancer Med*. 2017;6(6):1482–1489.
27. Degnim AC, Hoskin TL, Arshad M, et al. Alterations in the immune cell composition in premalignant breast tissue that precede breast cancer development. *Clin Cancer Res*. 2017;23(14):3945–3952.
28. McKian KP, Reynolds CA, Visscher DW, et al. Novel breast tissue feature strongly associated with risk of breast cancer. *J Clin Oncol*. 2009;27(35): 5893–5898.
29. Ghosh K, Vachon CM, Pankratz VS, et al. Independent association of lobular involution and mammographic breast density with breast cancer risk. *J Natl Cancer Inst*. 2010;102(22):1716–1723.
30. Figueroa JD, Pfeiffer RM, Brinton LA, et al. Standardized measures of lobular involution and subsequent breast cancer risk among women with benign breast disease: a nested case-control study. *Breast Cancer Res Treat*. 2016; 159(1):163–172.
31. Bourhis XD-L, Berthois Y, Millot G, et al. Effect of stromal and epithelial cells derived from normal and tumorous breast tissue on the proliferation of human breast cancer cell lines in co-culture. *Int J Cancer*. 1997;71(1):42–48.
32. Paraguassú-Braga FH, Borojevic R, Bouzas LF, Barcinski MA, Bonomo A. Bone marrow stroma inhibits proliferation and apoptosis in leukemic cells through gap junction-mediated cell communication. *Cell Death Differ*. 2003; 10(9):1101–1108.
33. Wang T, Xia D, Li N, et al. Bone marrow stromal cell-derived growth inhibitor inhibits growth and migration of breast cancer cells via induction of cell cycle arrest and apoptosis. *J Biol Chem*. 2005;280(6):4374–4382.
34. Ronnov-Jessen L, Petersen OW, Bissell MJ. Cellular changes involved in conversion of normal to malignant breast: importance of the stromal reaction. *Physiol Rev*. 1996;76(1):69–125.
35. Bissell MJ, Radisky D. Putting tumours in context. *Nat Rev Cancer*. 2001;1(1): 46–54.
36. Maffini MV, Soto AM, Calabro JM, Ucci AA, Sonnenschein C. The stroma as a crucial target in rat mammary gland carcinogenesis. *J Cell Sci*. 2004;117(8): 1495–1502.
37. Vinay KA, Nelson F, Aster JC. *Robbins and Cotran Pathologic Basis of Disease* 8th ed. Philadelphia, PA: Elsevier; 2010.
38. Gail MH, Brinton LA, Byar DP, et al. Projecting Individualized probabilities of developing breast cancer for white females who are being examined annually. *J Natl Cancer Inst*. 1989;81(24):1879–1886.

39. Tyrer J, Duffy SW, Cuzick J. A breast cancer prediction model incorporating familial and personal risk factors. *Stat Med*. 2004;23(7):1111–1130.
40. Tice JA, Cummings SR, Smith-Bindman R, Ichikawa L, Barlow WE, Kerlikowske K. Using clinical factors and mammographic breast density to estimate breast cancer risk: development and validation of a new predictive model. *Ann Intern Med*. 2008;148(5):337–347.
41. Barlow WE, White E, Ballard-Barbash R, et al. Prospective breast cancer risk prediction model for women undergoing screening mammography. *J Natl Cancer Inst*. 2006;98(17):1204–1214.
42. Chen J, Pee D, Ayyagari R, et al. Projecting absolute invasive breast cancer risk in white women with a model that includes mammographic density. *J Natl Cancer Inst*. 2006;98(17):1215–1226.
43. Louro J, Posso M, Hilton Boon M, et al. A systematic review and quality assessment of individualised breast cancer risk prediction models. *Br J Cancer*. 2019;121(1):76–85.
44. Sprague BL, Gangnon RE, Burt V, et al. Prevalence of mammographically dense breasts in the United States. *J Natl Cancer Inst*. 2014;106(10):dju255.
45. Busch SH, Hoag JR, Aminawung JA, et al. Association of state dense breast notification laws with supplemental testing and cancer detection after screening mammography. *Am J Public Health*. 2019;109(5):762–767.
46. Kerlikowske K, Sprague BL, Tosteson ANA, et al. Strategies to identify women at high risk of advanced breast cancer during routine screening for discussion of supplemental imaging. *JAMA Intern Med*. 2019;179(9):1230–1239.
47. McKinney SM, Sieniek M, Godbole V, et al. International evaluation of an AI system for breast cancer screening. *Nature*. 2020;577(7788):89–94.